15 September 1998

Optics Communications

ELSEVIER

Optics Communications 154 (1998) 307–312

Experimental evidence of selection and stabilization of spatial patterns in a CO_2 laser by means of spatial perturbations

M. Ciofini [a], A. Labate [a], R. Meucci [a,*], Peng-Ye Wang [b]

[a] *Istituto Nazionale di Ottica, Largo E. Fermi 6, 50125 Florence, Italy*
[b] *Laboratory of Optical Physics, Institute of Physics and Center for Condensed Matter Physics, Chinese Academy of Sciences, P.O. Box 603, 100080 Beijing, China*

Received 6 April 1998; accepted 9 June 1998

Abstract

We report on experimental evidence of selection and stabilization of unstable patterns by means of spatial perturbations. Thin metallic wires, with a diameter comparable to the laser wavelength, are inserted into a laser cavity to realize the selection and stabilization process. We studied the effects of small displacement of a single wire on the fundamental and annular patterns. The observed phenomena can be explained considering the diffractive effects of the wire inside the optical cavity. By using more wires instead of a single wire, square and hexagonal patterns are obtained. © 1998 Elsevier Science B.V. All rights reserved.

PACS: 2.65.Sf; 47.54.+r
Keywords: Optical pattern; Spatial perturbation; Diffraction

Considerable efforts have been recently devoted to stabilize spatio-temporal dynamics in non-linear sciences both theoretically and experimentally [1–11]. From the experimental point of view, great difficulties arise when one attempts to control a system involving both spatial and temporal coordinates.

However, just at the early development stages of laser physics, spatial effects due to diffraction by circular apertures were used for selecting high-order circular-symmetric modes in a He–Ne laser. Modes with azimuthal periodicity were isolated by means of two wires crossing the optical axis at appropriate angles [12,13].

In the last few years, interest in selection and stabilization of patterns in optical systems and lasers has been demonstrated by the proposal of several theoretical schemes, following the successful implementation of control of temporal chaos [14–21]. Martin et al. [10] proposed a Fourier space technique to stabilize, select and track unstable patterns. The same technique is the basis of the experimental work by Mamaev and Saffman [22]. Lu et al. [11] suggested an extension of the Pyragas method [23,24] which includes spatio-temporal feedback. The spatio-temporal feedback signal vanishes when the target pattern is reached. Recently, Lu et al. [25] theoretically demonstrated that a local feedback is effective to stabilize traveling waves in a spatially extended three-level laser model. Further control of extended optical systems combining spatial filtering with time-delayed feedback has been suggested in two recent papers [26,27] and such a procedure has been generalized to high dimensional systems whereby a pseudo space pattern emerges from a delayed dynamics [28]. In such a case, use is made of an adaptive control which generalizes the Pyragas method [29].

Most recently, Wang et al. [30] suggested a non-feedback method based on a weak spatial perturbation. By using this method, numerical simulations show that unstable rolls, squares and hexagons can be stabilized in an optical system. Similar to the non-feedback methods [31–38] for controlling temporal chaos, the spatial pertur-

* Corresponding author. E-mail: ric@ino.it

PII: S0030-4018(98)00333-2

bation method suggested by Wang at al. is much easier to implement in experiments for controlling spatio-temporal chaos. In an optical system, e.g. a laser, both the amplitude and phase of the optical field can be easily perturbed with absorptive or dispersive elements.

In this paper, we present a detailed experimental investigation of spatial perturbation effects produced by inserting thin metallic wires inside the cavity of a highly symmetric CO_2 laser. In the case of a single wire, it is possible to modify the type of symmetry breaking by varying the position of the wire, obtaining stabilization of different spatial patterns. We also show that, by using more wires with different geometries instead of a single wire, it is possible to select and stabilize square and hexagonal patterns.

The experimental apparatus is shown in Fig. 1. We use a CO_2 laser with a Fabry-Pérot cavity defined by a totally reflecting silicon flat mirror and a spherical ZnSe out-coupler (radius of curvature 5 m and reflectivity of 82%). The cavity length is 70 cm. The discharge column between the annular anode and cylindrical hollow cathode presents a high cylindrical symmetry along the laser axis. The discharge length is 40 cm. The active medium (CO_2 4.5%, He 82%, N_2 13.5%), at an average pressure of 23 mbar, is pumped by means of a high-voltage DC discharge in a pyrex tube with an internal diameter of 22 mm.

The most natural basis for such a cylindrical cavity is represented by Laguerre–Gauss modes [39–41]. These modes are described by the function:

$$A_{pli}(\rho,\varphi) = \frac{2}{\sqrt{\pi}}(2\rho^2)^{1/2}\left[\frac{p!}{(p+l)!}\right]^{1/2} \times L_p^l(2\rho^2)\,e^{-\rho^2} \times \begin{cases} \cos(l\varphi), & i=1 \\ \sin(l\varphi), & i=2 \end{cases}$$

where $p = 0,1,\dots$ is the radial index, $l = 0,1,\dots$ is the angular index, and i can take the values 1 and 2 corresponding to two similar modes shifted by $(\pi/2l)$. ρ is the radial coordinate normalized to the beam waist, φ is the angular coordinate, and L_p^l are the Laguerre polynomials of the indicated argument. The mode frequency in this basis only depends on the value of the index $q = 2p + l$. As a consequence, the mode degeneracy is $q + 1$ for each family with the same q.

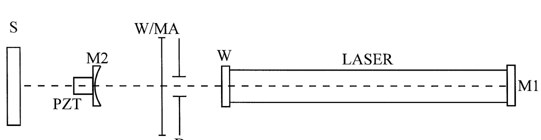

Fig. 1. Experimental setup. M1: total reflective plane mirror; W: ZnSe antireflection window; D: variable aperture diaphragm; W/MA: single wire or mask composed of metallic wires; M2: ZnSe out-coupling mirror (5 m radius of curvature) mounted on a piezo-electric translator (PZT); S: thermal image plate where the near-field of the pattern is monitored and recorded by means of a video camera connected to a frame-grabber PC card.

By varying the diameter of an intracavity iris, we are able to control the Fresnel number of the cavity and select different mode families. Moreover, we introduce a spatial perturbation by inserting a single thin metallic wire to spatially modulate the cavity loss parameter. The wire is located at 11 cm from the out-coupler mirror. The analysis for the effect of the single wire represents a clue to understand the effect of grids with more complicated geometries. Considering the fact that the diameter of the wire ($d = 100$ μm) and the laser wavelength ($\lambda = 10.6$ μm) are comparable, the Fraunhofer diffraction condition [42] ($z \gg \pi d^2/\lambda \cong 3.14$ mm, where z is the longitudinal coordinate) is satisfied at both mirrors of the laser cavity. The Fraunhofer diffraction pattern of a thin wire can be analytically obtained considering the wire as a one-dimensional rectangular function $\mathrm{rect}(x_1/d)$, where x_1 is the transverse coordinate perpendicular to the wire. The Fourier transform of this function along the x_0 axis at an observation distance z from the wire is $\mathrm{sinc}(dx_0/\lambda z)$. The width between the first two zeroes is $\Delta x_0 = 2(\lambda z/d)$. Hence, in our case, the width of the main lobe is 22 mm on the out-coupler mirror. Since the diameter of the fundamental mode on the same mirror is 5 mm, the effect of the wire is a weak spatial modulation. In fact, we have verified that the optical power reduction on the fundamental mode due to the insertion of the wire outside the optical cavity is about 4%. Inside the cavity, the spatial perturbation induces a weak transverse modulation which selects and stabilizes different laser output patterns depending on the symmetry of the perturbation.

First we consider the effect on the fundamental mode, as shown in Fig. 2a, obtained with a diaphragm aperture of 7.6 mm (Fresnel number of 2.0). If the wire crosses the optical axis, the power reduction is about 50% and the resulting output pattern displays two intensity lobes with a central line of zero intensity, as shown in Fig. 2b. In this case, the circular symmetry of the cavity is broken, but the cavity keeps inverse symmetry. There are two axes of inverse symmetry. One is the axis of the wire and the other is the axis perpendicular to the wire and passing through the center. Because of the inverse symmetry, the laser field on both axes will be mapped to the same axes by the cavity mirrors. Due to the Fraunhofer diffraction and the mapping effect, the cavity losses increase along the direction of the wire. Therefore, the laser radiation will be blocked along the wire and we obtain a laser pattern with two intensity lobes in the direction perpendicular to the wire. For the case where the wire has a displacement away from the center (a shift of the wire diameter is enough), inverse symmetry by the axis of the wire is broken. The laser field on this axis is not exactly mapped to the same axis in this case. Therefore, the wire-induced losses along

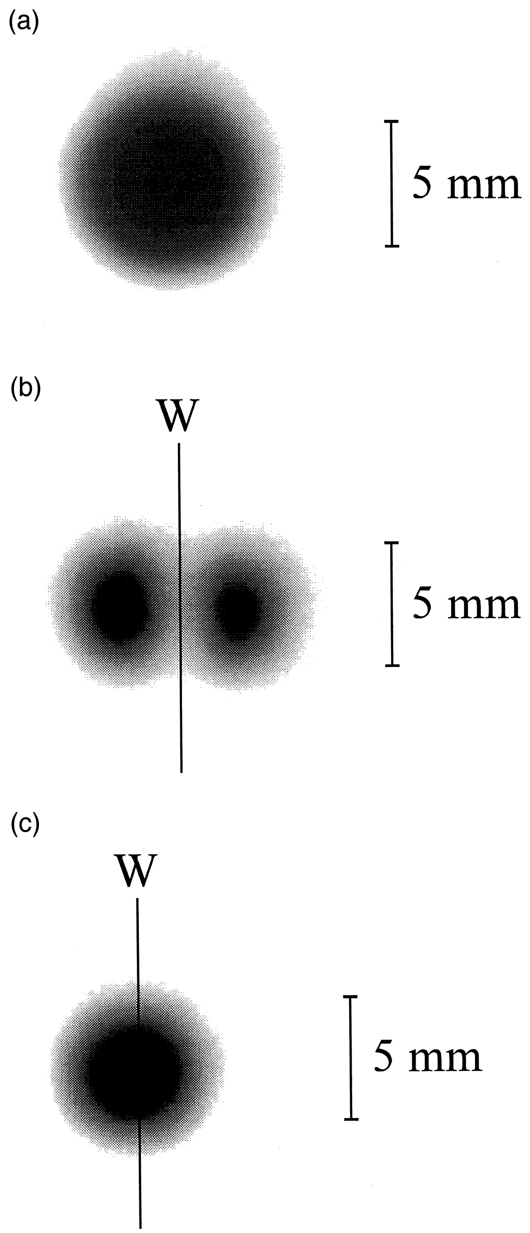

Fig. 2. (a) Transverse profile of the fundamental Gaussian mode imaged on a thermal plate located at 57 cm far from the out-coupling mirror. The output power is 310 mW. The laser is operated at a discharge current of 7.5 mA. The threshold current is 2.75 mA. (b) Transverse profile obtained after the insertion of a wire crossing the optical axis. The output power is 150 mW. (c) Recovered fundamental mode after a 200 μm displacement of the wire away from the optical axis. The output power is 150 mW.

the wire will be much smaller than those of the former case. As a consequence, in this case the pattern does not show regions of zero intensity, as shown in Fig. 2c. In other words, it is possible to recover the circular symmetry of the field distribution with such a small shift of the wire because the wire-induced losses are almost spatially uniform in this case.

A numerical analysis of the field propagation inside the optical cavity based on the Fox and Li algorithm [43] confirms the results of the role of the perturbation introduced by the wire. The transverse plane of the cavity is represented by a square grid consisting of 512×512 pixels (each one having a dimension of 50 μm). The geometrical parameters of the cavity have been chosen accordingly to the experimental ones. Fig. 3 summarizes the main results obtained. Fig. 3a shows the two lobe pattern when the wire crosses the optical axis, while Fig. 3b proves symmetry recovering when the wire is shifted by 600 μm far from the axis.

The considerations for the fundamental mode can be partly extended to the $q = 1$ family of Laguerre–Gauss modes, as shown in Fig. 4a, selected with a diaphragm aperture of 10.0 mm (Fresnel number of 3.5). Insertion of a wire crossing the optical axis determines the breaking of the unperturbed TEM_{01*} mode (the asterisk denotes two degenerate modes combined in space and in phase quadrature which form a circular symmetric mode) and the resulting mode appears as the TEM_{01}, as shown in Fig. 4b, with the two lobes aligned perpendicular to the wire. A displacement of the wire away from the axis of the cavity

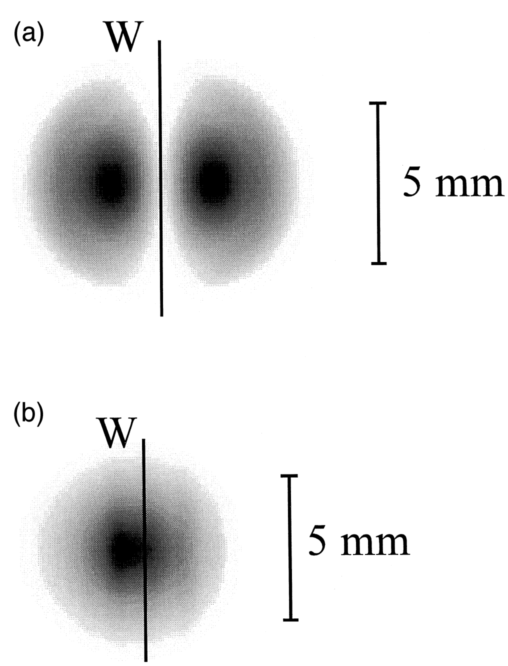

Fig. 3. Numerical results. (a) Two-lobe pattern obtained when the wire crosses the optical axis. (b) Pattern corresponding to a wire shift of 600 μm.

of 200 μm allows partial recovery of the symmetry of the unperturbed mode. In this case, the mode structure appears as a superposition of a weak annular pattern with a TEM_{10} mode with lobes aligned in the same direction of the wire, as shown in Fig. 4c. Further displacement of 100 μm determines cancellation of the weak annular contribution and the appearance of the TEM_{10} pattern oriented along the wire direction. In this way, it has been proved that the perturbation is able to fix the mode symmetry also in the direction of the wire, confirming the non-trivial role played by the wire in mode selection.

On the basis of our previous observations, the use of masks composed of more than one wire can lead to selection and stabilization of different kinds of elementary cells, as squares and hexagons, which are of great importance in pattern formation studies [44–46]. By using a mask composed of two perpendicular wires, we are able to stabilize the four-lobe pattern shown in Fig. 5a, when the aperture is 12 mm (Fresnel number of 5.1) and the two wires cross each other exactly on the optical axis. As in the case of a single wire, the situation changes if we move the crossing point of the two perpendicular wires out of the optical axis of the laser. A displacement of 250 μm of the crossing point results in a square pattern composed of nine intensity lobes, as shown in Fig. 5b. In both cases, the observed patterns are stable with respect to variations of the discharge current up to the laser threshold and the cavity detuning, controlled by the voltage applied to the piezo translator, for a frequency range corresponding to the free spectral range of the optical cavity $c/2L = 214$ MHz.

Another important elementary cell which can be stabilized in our system is a hexagon. In our experimental configuration, this elementary structure has been obtained by means of a mask of wires aligned along three directions making an angle of 60° with each other, the separation between parallel wires is 5 mm. Insertion of this mask selects and stabilizes the hexagonal pattern as shown in Fig. 6, up to the maximum Fresnel number of the cavity which is limited by the internal diameter of the discharge tube (Fresnel number of 17). Under this condition, introduction of the mask reduces the laser output power by a factor of 30%. Also for this pattern, which resembles the A_{031} and A_{032} Laguerre–Gauss modes, we observe that its shape remains unchanged if we approach the laser threshold by reducing the discharge current ($I_{th} = 4.5$ mA) or if we vary the cavity detuning. Another characteristic property of the hexagonal pattern is its stability with respect to the variation of the Fresnel number. The hexagonal pattern

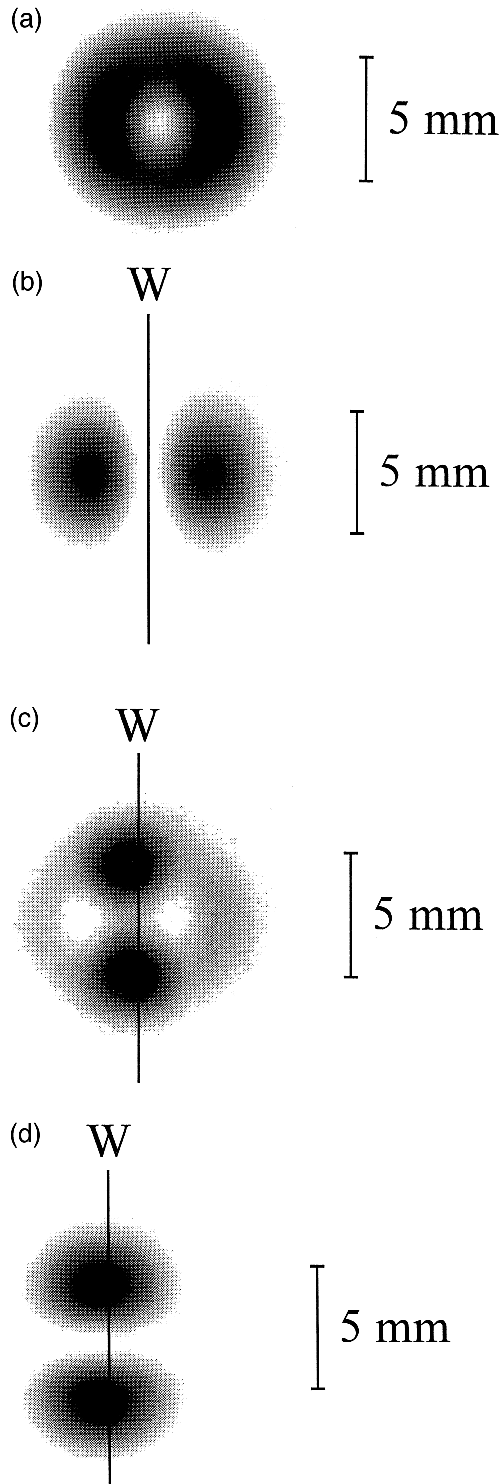

Fig. 4. (a) Unperturbed annular mode. The discharge current is 7.5 mA. The threshold current is 3.2 mA. The output power is 800 mW. (b) Output pattern after the insertion of a wire crossing the optical axis. The output power is 600 mW. (c) Output pattern after a 200 μm displacement of the wire away from the optical axis. The output power remains unchanged. (d) Output pattern after a further 100 μm displacement with respect to (c). The output power is 580 mW.

is stable up to a reduction of the diaphragm aperture to 11.5 mm (Fresnel number of 4.7), where the laser threshold is reached. Furthermore, by rotating the mask around the optical axis the hexagonal pattern follows the same motion.

In summary, we successfully selected and stabilized unstable patterns in a laser system by introducing intracavity spatial perturbations which break the cylindrical symmetry of the optical cavity. The spatial perturbation is realized by inserting thin metallic wires into the laser cavity. For the simple case of the fundamental and the annular modes perturbed by a single wire, the observed effects indicate that diffraction effects when $\lambda/d \cong 0.1$ inside the optical cavity play a crucial role in pattern selection. By using more wires and suitable masks, square and hexagonal patterns are selected and stabilized. They remain unchanged with respect to large variations of the discharge current (or the pump) and of cavity detuning.

(a)

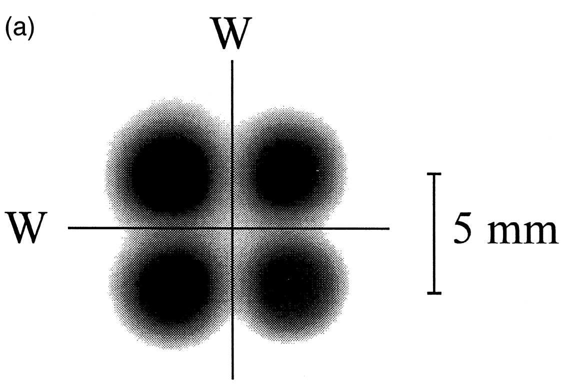

(b)

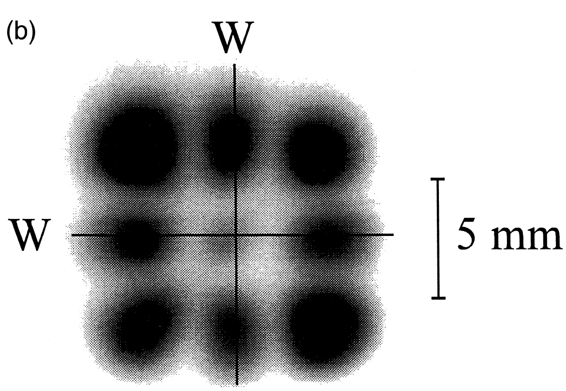

Fig. 5. (a) Output pattern obtained by inserting a mask composed of two perpendicular wires crossing the optical axis. The discharge current and output power are 7.5 mA and 380 mW, respectively. The unperturbed pattern is the A_{10} mode, with an output power of 940 mW. (b) Nine-lobe pattern obtained when the center of the mask is displaced 250 μm away from the optical axis. The output power is 460 mW.

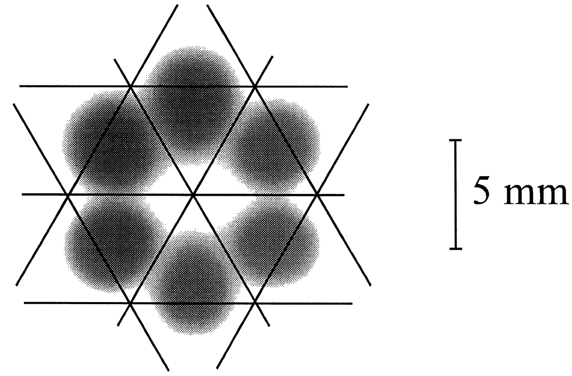

Fig. 6. Output pattern obtained after the insertion of the hexagonal mask as a spatial perturbation. The discharge current and the output power are 7.5 mA and 420 mW, respectively. The threshold discharge current is 4.5 mA. The corresponding unperturbed output power is 1400 mW.

Acknowledgements

Work partly supported by coordinated project 'Nonlinear Dynamics in Optical Systems' of the Italian National Council of Research and by the European Contract FM-RXCT960010 'Nonlinear Dynamics and Statistical Physics of Spatially Extended Systems'. The authors wish to thank Professor F.T. Arecchi for helpful discussions.

References

[1] J.A. Sepulchre, A. Babloyantz, Phys. Rev. E 48 (1993) 945.
[2] G. Hu, Z.L. Qu, Phys. Rev. Lett. 72 (1994) 68.
[3] D. Auerbach, Phys. Rev. Lett. 72 (1994) 1184.
[4] F. Qin, E.E. Wolf, H.C. Chang, Phys. Rev. Lett. 72 (1994) 1459.
[5] I. Aranson, H. Levine, L. Tsimring, Phys. Rev. Lett. 72 (1994) 2561.
[6] V. Petrov, S. Metens, P. Borckmans, G. Dewel, K. Showalter, Phys. Rev. Lett. 75 (1995) 2895.
[7] A. Hagberg, E. Meron, I. Rubinstein, B. Zaltzman, Phys. Rev. Lett. 76 (1996) 427.
[8] G.A. Johnson, M. Löcher, E.R. Hunt, Phys. Rev. E 51 (1995) R1625.
[9] C. Lourenço, M. Hougardy, A. Babloyantz, Phys. Rev. E 52 (1995) 1525.
[10] R. Martin, A.J. Scroggie, G.-L. Oppo, W.J. Firth, Phys. Rev. Lett. 77 (1996) 4007.
[11] W. Lu, D. Yu, R.G. Harrison, Phys. Rev. Lett. 76 (1996) 3316.
[12] W.W. Rigrod, Appl. Phys. Lett. 2 (1963) 51.
[13] W.W. Rigrod, in: P. Grivet, N. Bloemberger (Eds.), Eletronique Quantique, Proc. 3rd. Int. Conf. of Quantum Electronics, Paris, February 1963, Dumond, Paris, 1964, p. 1285.

[14] E. Ott, C. Grebogi, J.A. Yorke, Phys. Rev. Lett. 64 (1990) 1196.
[15] W.L. Ditto, S.N. Rauseo, M.L. Spano, Phys. Rev. Lett. 65 (1990) 3211.
[16] U. Dressler, G. Nitsche, Phys. Rev. Lett. 68 (1992) 1.
[17] B. Peng, V. Petrov, K. Showalter, J. Phys. Chem. 95 (1991) 4957.
[18] E.R. Hunt, Phys. Rev. Lett. 67 (1991) 1953.
[19] R. Roy, T.W. Murphy, T.D. Maier, Z. Gills, E.R. Hunt, Phys. Rev. Lett. 68 (1992) 1259.
[20] S. Bielawski, M. Bouazaoui, D. Derozier, P. Glorieux, Phys. Rev. A 47 (1993) 3276.
[21] P. Parmananda, P. Sherard, R.W. Rollins, H.D. Dewald, Phys. Rev. E 47 (1993) R3003.
[22] A.V. Mamaev, M. Saffman, Phys. Rev. Lett. 80 (1998) 3499.
[23] K. Pyragas, Phys. Lett. A 170 (1992) 421.
[24] K. Pyragas, A. Tamasevicius, Phys. Lett. A 180 (1993) 99.
[25] W. Lu, D. Yu, R.G. Harrison, Phys. Rev. Lett. 78 (1997) 4375.
[26] M.E. Bleich, D. Hochheiser, J.V. Moloney, J.E.S. Socolar, Phys. Rev. E 55 (1997) 2119.
[27] D. Hochheiser, J.V. Moloney, J. Lega, Phys. Rev. A 55 (1997) R4011.
[28] S. Boccaletti, D. Maza, H. Mancini, R. Genesio, F.T. Arecchi, Phys. Rev. Lett. 79 (1997) 5246.
[29] S. Boccaletti, F.T. Arecchi, Europhys. Lett. 31 (1995) 127.
[30] P.-Y. Wang, P. Xie, J.-H. Dai, H.-J. Zhang, Phys. Rev. Lett. 80 (1998) 4669.
[31] R. Lima, M. Pettini, Phys. Rev. A 41 (1990) 726.
[32] Y. Braiman, I. Goldhirsch, Phys. Rev. Lett. 66 (1991) 2545.
[33] A. Azevedo, S.M. Rezende, Phys. Rev. Lett. 66 (1991) 1342.
[34] L. Fronzoni, M. Giocondo, M. Pettini, Phys. Rev. A 43 (1991) 6483.
[35] R. Chacón, J. Díaz Bejarano, Phys. Rev. Lett. 71 (1993) 3103.
[36] R. Meucci, W. Gadomski, M. Ciofini, F.T. Arecchi, Phys. Rev. E 49 (1994) R2528.
[37] V.N. Chizhevsky, R. Corbalan, A.N. Pisarchick, Phys. Rev. E 56 (1997) 1580.
[38] P. Colet, Y. Braiman, Phys. Rev. E 53 (1996) 200.
[39] H. Kogelnik, in: A.K. Levine (Ed.), Lasers: A Series of Advances, Vol. 1, Dekker, New York, 1966, p. 295.
[40] H. Kogelnik, T. Li, Appl. Opt. 5 (1966) 1550.
[41] A.E. Siegman, Lasers, University Series Books, Mill Valley, CA, 1986, Chap. 16, p. 647.
[42] J.W. Goodman, Introduction to Fourier Optics, McGraw–Hill, San Francisco, CA, 1968, Chap. 4, p. 61.
[43] A.G. Fox, T. Li, Bell System Tech. J. 40 (1961) 453.
[44] N.B. Abraham, W. Firth, (Eds.), Special issues on Transverse Effects in Nonlinear Optical Systems, J. Opt. Soc. Am. B 7 (Nos. 6 and 7), June and July 1990.
[45] F.T. Arecchi, Physica D 86 (1995) 297, and references therein.
[46] W. Lange, A. Aumann, T. Ackemann, E. Büthe, Quantum Semiclass. Optics 10 (1998) R23.